Microwave-assisted one-step patterning of aqueous colloidal silver

2012 Nanotechnology 23 265302

(http://iopscience.iop.org/0957-4484/23/26/265302)

Nanotechnology **23** (2012) 265302 (7pp) doi:10.1088/0957-4484/23/26/265302

Microwave-assisted one-step patterning of aqueous colloidal silver

G Yang[1], Y W Zhou[1], Z R Guo[2], Y Wan[1], Q Ding[1], T T Bai[1], C L Wang[1] and N Gu[1]

[1] State Key Laboratory of Bioelectronics and Jiangsu Key Laboratory for Biomaterials and Devices, Southeast University, Nanjing 210096, People's Republic of China
[2] The Second Affiliated Hospital of Nanjing Medical University, Nanjing 210011, People's Republic of China

E-mail: guning@seu.edu.cn (N Gu)

Received 11 March 2012, in final form 10 May 2012
Published 15 June 2012
Online at stacks.iop.org/Nano/23/265302

Abstract
A new approach of utilizing microwave to pattern gradient concentric silver nanoparticle ring structures has been presented. The width and height of a single ring and the space between adjacent rings can be adjusted by changing the silver colloidal concentration and the microwave output power. By simply enhancing the ambient vapour pressure to the saturated value during microwave-assisted evaporation, sub-100 nm rings can be deposited in between adjacent micro-rings over a distance of millimetres. Combined with microwave sintering, this approach can also create conductive silver tracks in a single step, showing huge potential in fabricating micro- and nano-electronic devices in an ultra-fast and cost-effective fashion.

S Online supplementary data available from stacks.iop.org/Nano/23/265302/mmedia

(Some figures may appear in colour only in the online journal)

1. Introduction

Well-defined nanostructures have found potential applications in photonics [1], electronics [2], biotechnology [3] etc. Therefore, several state-of-the-art strategies such as deep ultraviolet (UV) and extreme UV photolithography, electron-beam writing and ion-beam lithography have been developed [4]. On the other hand, continuous efforts have been made to explore alternative nanostructure fabrication approaches regarding the cost-effectiveness and throughput. As a non-conventional patterning technique, evaporation-induced self-assembly (EISA) of non-volatile solute has received much attention, owning to the ease and low cost of producing large area intricate patterns [5, 6]. However, the yielded structures are often stochastically organized without desired regularity because of the instabilities in the evaporation process [5]. Several elegant methods have been exploited to exert precise control over the evaporation-induced feature morphology [7]. Among these, template-based EISA can site-specifically arrange nanoparticles into the sub-100 nm scale [8]. However, the pre-fabrication of templates inevitably increases the processing steps and cost [9]. Template-free EISA strategies have also been explored, with two representatives being dip coating EISA [10] and confined geometry EISA [11–17]. Compared with the former, the triple line moving velocity of the drying solvent, which is critical in controlling the size, spacing and periodicity of the resulting patterns [18, 19], cannot be flexibly tailored for the confined geometry configuration. Despite the delectable development of various control approaches, to date, the capability of creating features on a scale below 100 nm is still a major challenge for EISA.

As a non-invasive and time-saving processing tool, microwave has been widely used in synthesizing nanomaterials [20–23]. Because of its unique properties, such as rapid volumetric and uniform heating [22], microwave provides scale-up processes with a uniform reaction environment, thus paving the way to the large-scale industrial production of high-quality nano-materials. Although utilizing microwave to assist nano-self-assembly during synthesis is possible [23, 24], it is more common to arrange nano-building blocks directly from their suspension stock

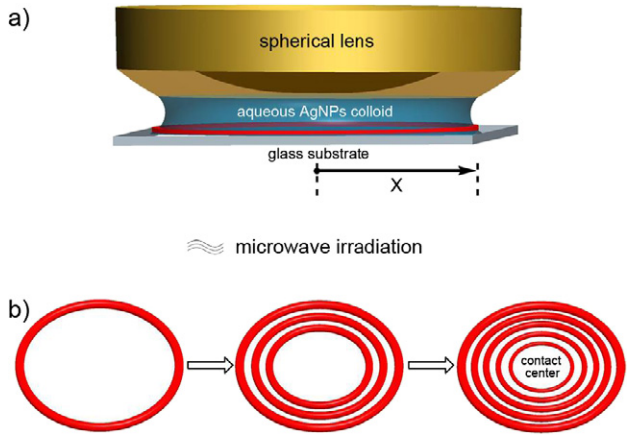

Figure 1. Schematic illustration of AgNPs assembling into gradient concentric rings. (a) The experimental setup: a drop of colloidal silver was trapped in a sphere-on-flat geometry, forming a capillary bridge. Under microwave irradiation, as the solvent evaporated, the initial AgNPs ring was deposited at the perimeter of the droplet (denoted as the red circle). '*X*' is defined as the radical distance away from the sphere/glass contact centre. (b) Stepwise representation of the formation of gradient concentric rings propagating from the capillary edge to the sphere/glass contact centre during solvent evaporation (top view).

with subsequent patterning processes [10]. Note that the evaporative instabilities (e.g. 'Rayleigh–Benard' flow) inside the drying solvent often result from the temperature gradient [16], while microwave imparts heat to the system uniformly due to the simultaneous excitation of the dipole moment of polar molecules [25] (e.g. water molecules), which can kerb the temperature gradient, we thus reason that it might be possible to utilize microwave as a powerful tool to design a new patterning approach (see supporting information section 1 available at stacks.iop.org/Nano/23/265302/mmedia). However, to the best of our knowledge, until now few studies have reported the microwave-assisted evaporative patterning of colloidal nanoparticles (NPs), especially from the aqueous solution [26].

Herein, we report a facile approach of employing microwave irradiation to regulate EISA of aqueous silver NPs (AgNPs) in a confined geometry composed of a spherical lens and a glass substrate (i.e. sphere-on-flat), as illustrated in figure 1. The patterns formed on the glass substrate are hundreds of gradient concentric rings, with width ranging from micrometres to nanometres. The specific geometry of the rings feature, including the width (ω) and height (h) of the individual ring and the centre-to-centre distance between two adjacent rings (λ_{c-c}), could be controlled by varying solution concentration and the applied microwave power density. Moreover, measurements of the electric properties of the patterns reveal that, by allying microwave-assisted EISA and microwave sintering, arrays of conductive discontinuous metallic NPs structures with high regularity can be deposited in a single step, showing the huge potential in fast electronic detection of biological and chemical molecules [3, 27].

2. Experimental details

2.1. Materials preparation

Polyvinyl alcohol (PVA, 31 000 MW), $NaBH_4$ and $AgNO_3$ were purchased from Sigma Aldrich. Millipore-quality water (18.25 MΩ cm^{-1}), prepared with a Milli-*Q* Plus water system, was used throughout the experiments. All experiments with Ag^+ were carried out under low light conditions and 23–26 °C temperature. The spherical lenses and glass slides were cleaned by using a mixture of sulfuric acid and Nochromix. Subsequently they were rinsed with Millipore-quality water extensively and blow-dried with N_2.

2.2. AgNPs fabrication

AgNPs were prepared in aqueous solutions using wet chemical reduction methods. Conventionally, AgNPs were synthesized by $NaBH_4$ reduction: to an aqueous $AgNO_3$ solution (300 μl; 0.35 M), PVA (40 ml; 0.5 wt%) was added as protective agent. During the whole process, synthesis was carried out under 1500 rpm mix. After this mixing to homogenize Ag^+ and PVA solutions, aqueous $NaBH_4$ solution (100 μl; 0.1 M) was added dropwise to reduce the metal salts, forming the desired nanoparticles. Before each experiment, the as-prepared colloidal silver was centrifuged (Eppendorf, Centrifuge 5804R) and washed by Millipore-quality water three times to remove excessive agents. The Ag content in the final colloid was about 25.0 μg ml^{-1}. The as-prepared silver colloid was then diluted by using Millipore-quality water to 20.0 μg ml^{-1}, 15.0 μg ml^{-1} and 10.0 μg ml^{-1}, respectively. Before each experiment, the sample was ultrasonically dispersed for 10 min.

2.3. Patterning of AgNPs

The confined geometry was composed of a spherical upper surface and a flat glass slide, as illustrated in figure 1(a). Both the spherical upper surface and the glass substrate were firmly fixed at the top and bottom of the sample holders, respectively. A drop of 50 μl as-prepared silver colloid (25.0 μg ml^{-1}) was then injected and trapped between the spherical lens and the glass substrate by capillary force. The upper spherical lens was then brought into contact with the lower glass substrate. Subsequent microwave irradiation with three different local power densities (40, 80 and 120 mW cm^{-2}) was applied (Glanz, G80F23DCSL-F7(R0)). To research on colloidal concentration effect, silver colloids with different concentrations (20.0, 15.0 and 10.0 μg ml^{-1}) were evaporated under microwave (80 mW cm^{-2}). Control experiments were set as follows. After loading the colloidal silver (25.0 μg ml^{-1}) into the confined geometry, Group 1 was kept at room temperature (25 °C) while Group 2 was heated by using the traditional method (65 °C, Omron E5CZ) until the droplets were thoroughly evaporated. After drying, patterns on the glass substrate were evaluated.

2.4. Characterization

The resulting patterns were characterized by a Zeiss Axioskop 40 optical microscope in the transmittance mode and with scanning electron microscopy (SEM, Carl Zeiss, Ltd). AFM images of the featured morphology of the patterns formed on the glass surface were performed using a scanning force microscope in tapping mode (SFM, Pico Scan TM 2500).

2.5. Electric properties measurements

A pre-designed mask was coated on the AgNPs rings at $X = 7000$ μm. Pt electrodes were deposited using a vacuum sputtering method (Quorum, Q150TS; 40 mA; 10 min). The mask was then removed and the part of the pattern under measurement was scratched apart from the global rings (figure 5(a)). The current–voltage responses were measured using a semiconductor analyser with four-probe configuration (Micro Manipulator, Ltd).

3. Results and discussion

When evaporated under microwave irradiation, AgNPs were carried to the perimeter by the radical capillary flow, which compensated for the maximum solvent evaporation loss at the capillary edge, and were deposited to create a local roughness (i.e. the contact line was 'pinned') [16]. Continuous evaporative loss of water at the capillary edge rendered the reduction of the contact angle to the critical value where the excess free energy of the drop prevailed over the pinning potential [28] (supporting information section 1.1 available at stacks.iop.org/Nano/23/265302/mmedia), and the contact line was dragged to the next pinning site towards the sphere/glass contact centre (figure 1(b)) (i.e. the contact line 'slipped'), leading to the release of the excess free energy. Thus, one cycle of 'stick–slip' motion of the contact line was finished. Continuous input microwave energy guaranteed that the excess free energy condition was satisfied at each 'stick–slip' cycle. The repeated 'stick–slip' motions of the contact line created concentric rings composed of AgNPs with high degree of order over a distance of thousands of micrometres (supporting information, figure S5 available at stacks.iop.org/Nano/23/265302/mmedia). A typical optical microscopic picture of a small region of the entire rings is shown in figure 2. Locally, the periodic rings appear as parallel strips. This pattern is a direct proof that under microwave irradiation within the sphere-to-plate geometry, aqueous colloidal AgNPs aggregate through the controlled, repetitive pinning and depinning cycles of the three phase contact line (figure 1(b)) into highly ordered periodic rings.

Representative atomic force microscopy (AFM) measurements of AgNPs rings at different radical distances (figure 3) revealed their progressively changing sizes and spacing along with the contact line shrinking towards the centre of the sphere/glass contact, regardless of the variation of the microwave output power.

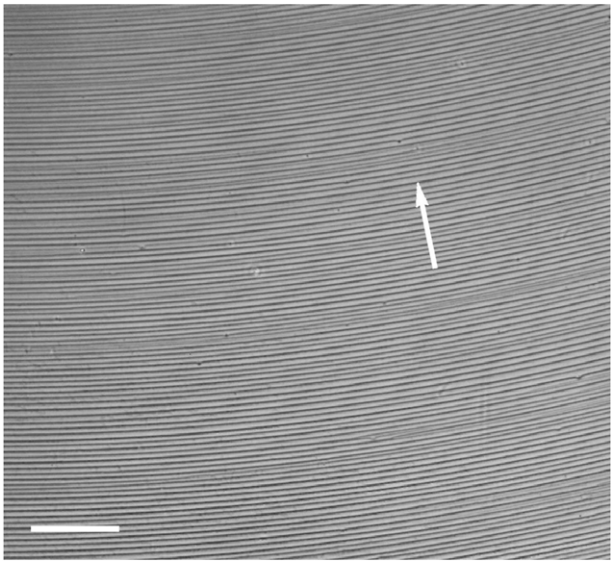

Figure 2. Optical microscopic picture of the gradient concentric AgNPs rings. The local power density of the applied microwave irradiation was 120 mW cm^{-2}. The white arrow indicates the receding direction of the contact line. The scale bar is 100 μm.

The evaporation took ~1 h to complete for 40 mW cm^{-2} (local power density) microwaves. The average temperature maintained at 42 °C. The width of the ring, ω, the height of the ring, h, and the centre-to-centre distance between adjacent rings, λ_{c-c}, progressively decreased from $\omega = 5.92$ μm, $h = 147.3$ nm and $\lambda_{c-c} = 10.0$ μm at $X = 8400$ μm (figure 3(a)) to $\omega = 2.93$ μm, $h = 61.8$ nm and $\lambda_{c-c} = 5.89$ μm at $X = 7000$ μm (figure 3(b)) and to $\omega = 2.1$ μm, $h = 39.3$ nm and $\lambda_{c-c} = 44.8$ μm at $X = 5600$ μm (figure 3(c)). The associated circumference of the ring was roughly four orders of magnitude larger than ω (e.g. $(2\Pi \times X)/\omega = 2\Pi \times 5600$ μm$/2.1$ μm $\sim 1.7 \times 10^4$; corresponding to the rings pattern shown in figure 3(c)). Because this periodic rings pattern may have potential usage in micro-optical gratings, it should be of importance in adjusting the relative dimension parameters (ω, h and λ_{c-c}). The resulting patterns in figures 3(d)–(i) reveal a noteworthy influence of the microwave output power on the consequent dimensions of the AgNPs rings. When microwave with local power density of 80 mW cm^{-2} was applied (evaporation time ~40 min, average temperature 55 °C), the ring width and height decreased $\omega = 4.2$ μm, $h = 99.8$ nm at $X = 8400$ μm (figure 3(d)), $\omega = 2.6$ μm, $h = 60.6$ nm at $X = 7000$ μm (figure 3(e)) and $\omega = 1.9$ μm, $h = 39.3$ nm and at $X = 5600$ μm (figure 3(f)), while the centre-to-centre distance went up at each position ($\lambda_{c-c} = 12.8$ μm, $\lambda_{c-c} = 8.3$ μm and $\lambda_{c-c} = 6.3$ μm at corresponding positions). This trend was continued when using the 120 mW cm^{-2} microwave irradiation (average temperature ~70 °C). The drying time was shortened to 21 min. The centre-to-centre space, λ_{c-c}, increased to 13.7 μm at $X = 8400$ μm (figure 3(g)), to 11.5 μm at $X = 7000$ μm (figure 3(h)) and to 9.3 μm at $X = 5600$ μm (figure 3(i)). However, the width (ω) and the height (h) of the individual ring decreased to 1.9 μm and 78.3 nm at $X = 8400$ μm, to 1.4 μm and 48.8 nm at $X =$

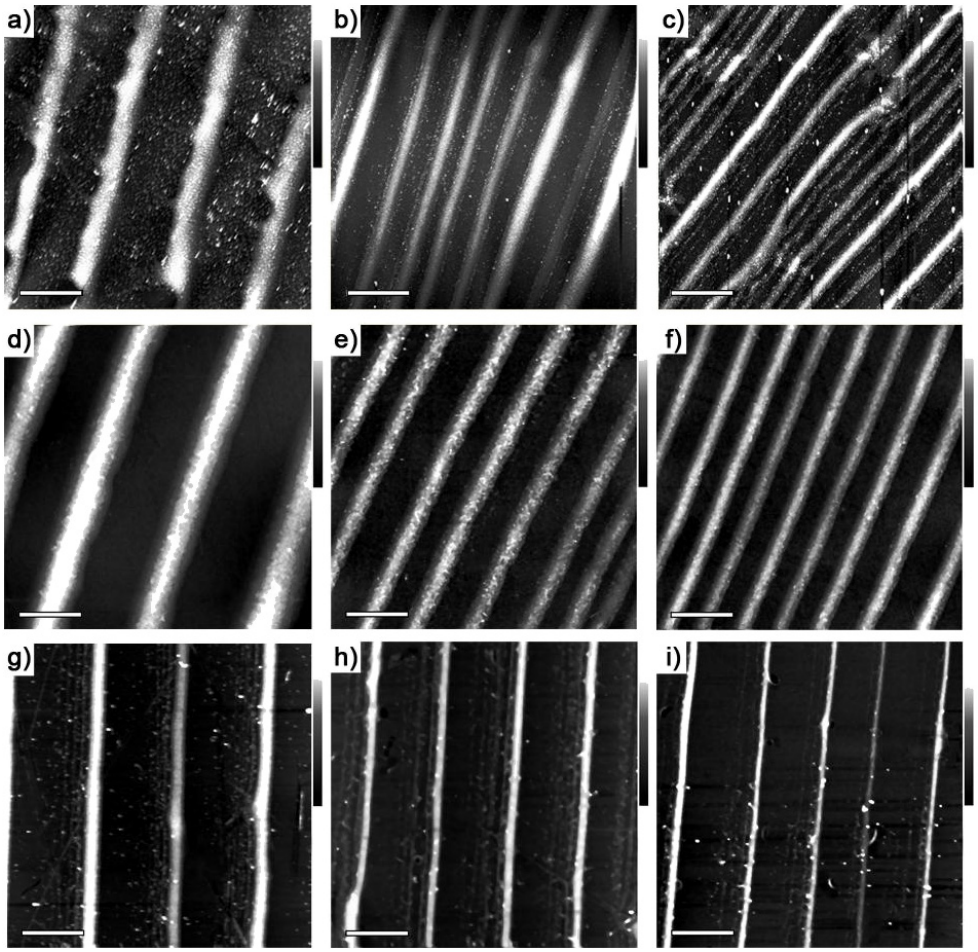

Figure 3. AFM height images of the surface patterns formed on the glass substrate at different radical positions as the contact line progressively approaches the centre of the sphere/glass contact with (a)–(c) 40 mW cm^{-2}, (d)–(f) 80 mW cm^{-2} and (g)–(i) 120 mW cm^{-2} microwaves. The scale bar is 10 μm for all images. The Z scale is 220 nm for (a), 150 nm for (d), 100 nm for (g), 80 nm for (b) and (c) 70 nm for (e) and (h) and 50 nm for (f) and (i).

7000 μm and to 0.9 μm and 35.3 nm at $X = 5600$ μm. The possible explanation of the microwave power density effect could be as follows: with the increase of the local microwave power density, the time needed for the excess free energy surpassing the pinning potential at each cycle was shortened, so that the duration of each 'stick' event went down, leading to fewer AgNPs deposited (i.e. the ring width and height decreased); meanwhile, higher microwave power density means larger moving velocity of the contact line and the accelerated moving velocity of the contact line resulted in a larger 'slip' distance and eventually larger centre-to-centre distance of adjacent rings. The trend resulting from the microwave power density effect is different from the concentration effect observed in our experiment (supporting information, section 3 available at stacks.iop.org/Nano/23/265302/mmedia) and copious previous studies [29] where all three parameters (ω, h and λ_{c-c}) decreased with reduced solution concentration if the evaporation rate was fixed (i.e. drying at constant temperature).

Although the sphere-on-flat geometry has been utilized to regulate ELSA of colloidal nanoparticles before [30], the evaporation rate of the liquid materials and the consequent moving velocity of the contact line, which is crucial in controlling the size, spacing and periodicity of the resulting patterns, could not be effectively changed.

By employing the microwave local power density effect here, the scope of the ways controlling over the relative dimensions of the patterns would be extended. In addition, the solvent used in previous work was volatile organic media (e.g. toluene). As a non-volatile solvent, water evaporates too slow at room temperature (i.e. the excess free energy condition cannot be met without the energy input) so that almost all the solute is transferred by the convective capillary flow to the droplet edge where only a single ring was deposited (figure 4(a)) [31]. On the other hand, the traditional heating method is able to fulfil the excess free energy condition so that multirings can be created (figure 4(b)), yet without the desired dimensions and regularity. The single ring width and the space between adjacent rings are several tens of micrometres. That is because energy transferred under this condition is not as efficient as microwave heating (for drying time, 6 min more than needed in microwave-assisted evaporation). During each 'stick–slip' cycle, the drop needs more time to accumulate free energy before the contact line 'slips'. So the contact

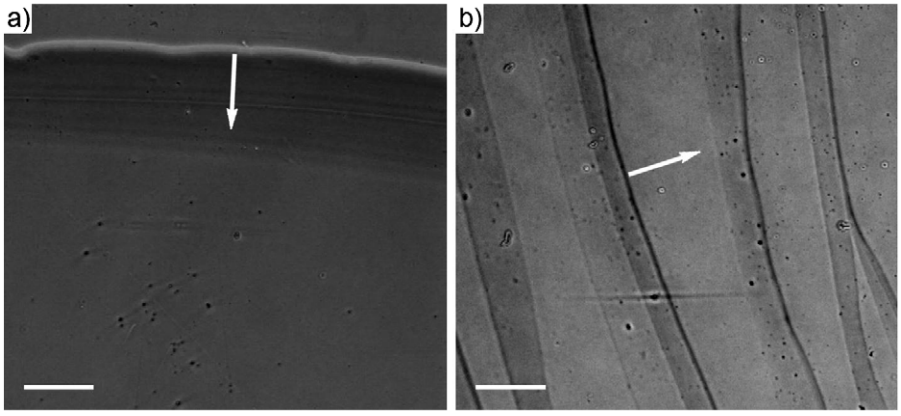

Figure 4. Optical microscopic images of the patterns formed from the EISA of the aqueous colloidal silver in the confined geometry without microwave irradiation. (a) Evaporated at room temperature (25 °C), only a single ring was deposited at the initial pinning position. (b) When heating from the bottom (∼70 °C), irregular multirings were obtained due to the temperature gradient driven hydrodynamic convective flow within the drying droplet. The scale bar is 100 μm for both images. The white arrow indicates the receding direction of the contact line.

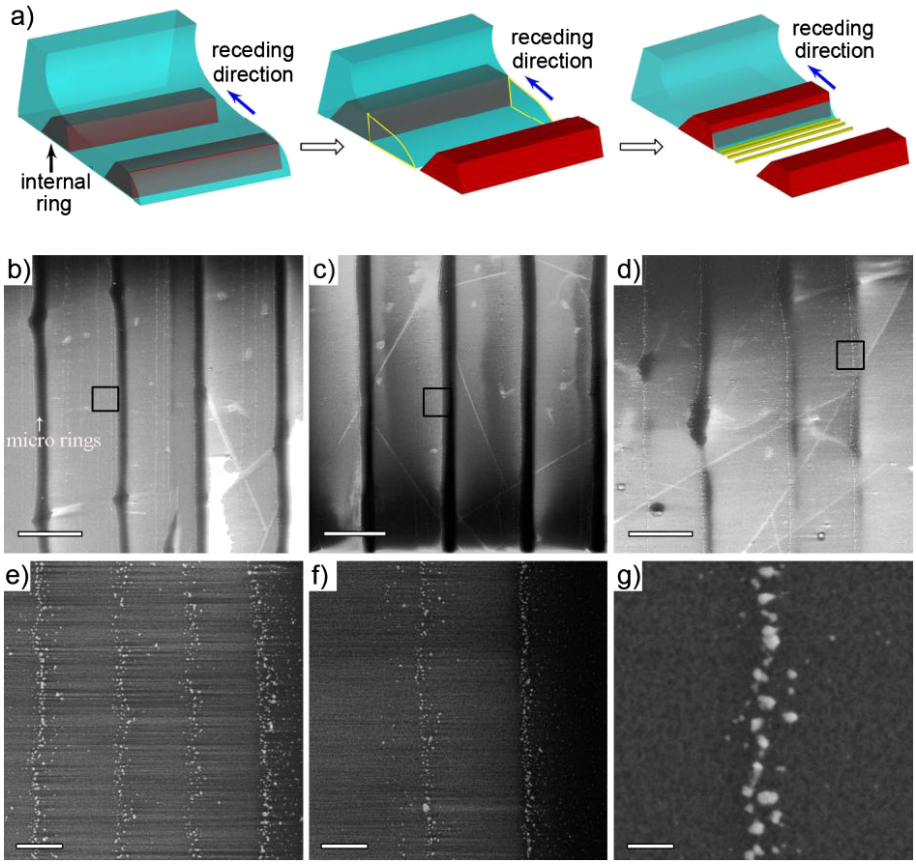

Figure 5. (a) Schematic illustration of the interspaced nanoscale ring formation within two adjacent micro-rings. At the capillary edge, the internal ring has been deposited at the next pinning position before the contact line 'slips' (left panel). A wedge-like thin water film (dashed yellow frame) is trapped because of the pre-deposited ring when the contact line moves to the next pinning position (middle panel). As evaporating, the wedge-like water film goes through 'stick–slip' cycles to leave nanoscale interspaced rings (right panel). (b)–(d) A set of SEM images of the surface patterns as the contact line progressively shrinks to the centre of the sphere/glass contact. The scale bar is 10 μm for (b) and 5 μm (c) and (d). (e)–(g) SEM images of the detailed structure of interspaced nanoscale rings at the corresponding positions marked with black open squares in (b)–(d). The scale bar is 500 nm for (e) and (f) and 100 nm for (g).

line is pinned longer and more AgNPs accumulate at the edge, causing larger ring width. At the same time, the pinning potential is improved by an increased number of AgNPs deposited at the edge, so that the drop needs more excess free energy to conquer the pinning potential. Eventually the contact line 'slips' more to reach the next pinning site and so

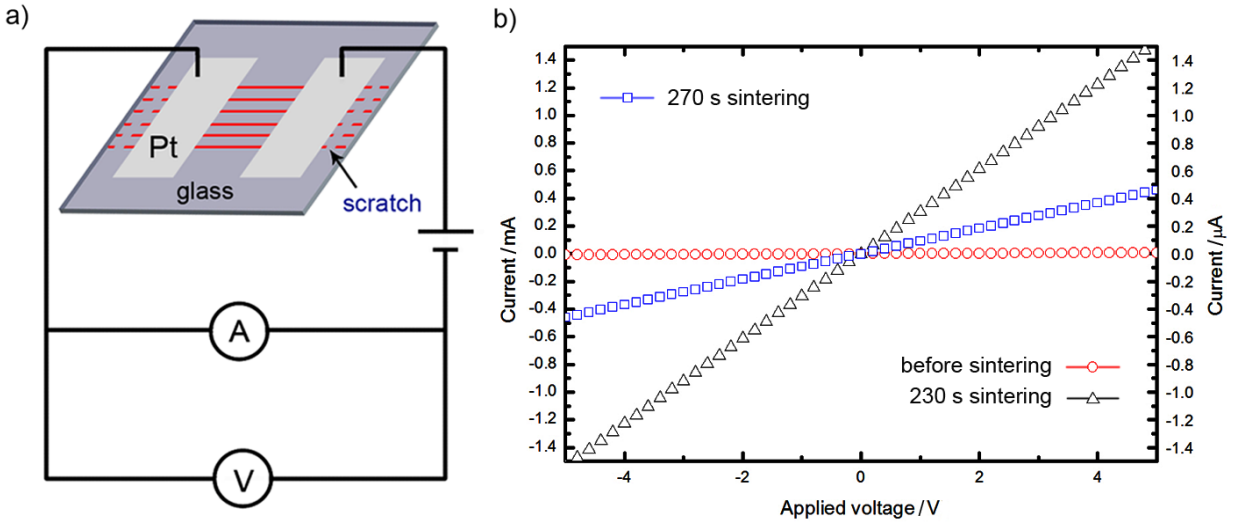

Figure 6. Electric property measurements of AgNPs rings. (a) Schematic illustration of conductance measurement for periodic AgNPs rings. (b) Current–voltage response of the AgNPs rings before sintering (red open circles), 230 s microwave sintering (black open triangles) and 270 s microwave sintering (blue open squares).

the space between adjacent rings is increased. The irregularity is due to the vertical temperature gradient resulting from bottom heating, which causes the evaporative instability [16]. The control experiments indicate, by only employing the confined geometry without the assistance of microwaves, that aqueous colloidal AgNPs cannot be assembled with the desired regularity.

From the perspective of hydrodynamics, microwave meets the excess free energy condition without giving rise to a vertical temperature gradient (uniform heating feature). Besides, we notice that microwave irradiation may also strengthen the evaporative flux (supporting information, section 4 available at stacks.iop.org/Nano/23/265302/mmedia), which kerbs the 'Marangoni effect' and further stabilizes the contact line, facilitating the precipitation of the AgNPs into a rings structure [19, 32]. The confined geometry was then coated with a polyresin (transparent to microwave energy) vessel with only a small hole at the top to retain more highly saturated vapour. 120 mW cm^{-2} microwave was applied. Ordered sub-100 nm rings were formed in between adjacent micro-rings over a distance of millimetres. A set of SEM images is shown in figures 5(b)–(g). As the evaporation front moved towards the contact centre, the average number of interspaced nano-rings within adjacent micron rings gradually reduced from four at $X = 8400$ μm (figures 5(b) and (e)), to three at $X = 6300$ μm (figures 5(c) and (f)), and to one at $X = 4200$ μm (figures 5(d) and (g)). No interspaced rings were observed at $X < 4000$ μm (figure S9 available at stacks.iop.org/Nano/23/265302/mmedia). The nanoscale rings had ultra-high aspect ratio (e.g. ω: $(2\Pi \times X) =$ 50 nm:$2\Pi \times 4200$ μm $\sim$ 1:5.3 $\times$ 10^5 at $X = 4200$ μm). It is noteworthy that these nanoscale rings were, for the first time, achieved by EISA in a sphere-on-flat geometry [13, 16].

The interspaced rings within two adjacent micron rings were also arranged in a gradient manner, which can be attributed to the contact line dynamics of precipitation in the drop interior before it slips [33]: In the meniscus, before the contact line cracks from the deposited ring, an internal ring has already been created by the stagnation flow at the next contact line pinning position (figure 5(a) left panel). When the contact line 'slips' to the new pinning position, a wedge-like water layer is held by the newly formed ring (figure 5(a) middle panel). This wedge-like water layer again experiences repetitive 'stick–slip' motion, leaving interspaced nano-rings behind (figure 5(a) right panel).

Control experiments indicated that the interspaced rings were sensitive to the evaporative flux. They only appeared when the ambient vapour pressure was close to the saturated value (e.g. 70 °C, 31.2 kPa for water). With ambient vapour pressure far from the saturated value, AgNPs between two adjacent micro-rings were stochastically arranged (figure S10 available at stacks.iop.org/Nano/23/265302/mmedia).

Further electric properties of the resulting patterns were evaluated. Figure 6 shows the conductance measurements of AgNPs rings. Two Pt electrodes were deposited at the intermediate region ($X = 5600$ μm) with pre-determined scales (see section 2). The current–voltage response (figure 6(b)) of the AgNPs rings pattern is linear within the voltage range of $\pm$0.2 V, yielding a characteristic feature of a one-dimensional conductor. The resistivity value was calculated at 0.8 Ω m, about seven orders larger than that of the bulk silver (1.5×10^{-8} Ω m). The origin of the high resistivity lies in the organic coating agent (i.e. PVA) of AgNPs. Note that the average height of the rings, 35.3 nm, is within the microwave penetration depth into silver (1.3 μm) [34], it is reasonable to use microwave irradiation to sinter the as-prepared AgNPs rings to reduce the resistivity.

After a hundred seconds of high power microwave sintering (510 mW cm^{-2}), the resistivity of AgNPs rings was decreased by four orders at most (microwave sintering for 270 s). The resistivity as a function of the microwave sintering time was also illustrated (figure S11 available at stacks.iop.org/Nano/23/265302/mmedia). The optimized resistivity of the AgNPs rings obtained was 1.2×10^{-5} Ω m, about three

orders of magnitude higher than that of the bulk silver, but can be comparable to that of the NP arrays prepared using other methods [35]. Efforts aimed at exploring the electronic chemical and biological sensing properties of thus-made patterns are underway.

It should be noted that by combining the microwave-assisted patterning with the microwave sintering (i.e. a programmable microwave process), a large area of conductive pattern of AgNPs rings can be obtained in less than half an hour without any further physical or chemical processing, demonstrating that this green approach is extremely simple, cheap and time-effective, yielding a potential application in fabricating micron and nano-electronic devices on an industrial scale.

4. Conclusion

In summary, we have demonstrated a facile, one-step and template-free approach, microwave-assisted evaporation-induced self-assembly, to deposit regular concentric ring features from aqueous nanoparticle colloid. The ring size and spacing could be controlled by tuning the colloidal concentration and local power density of the microwave. This technique opens up a new avenue to fabricate large arrays of one-dimensional nanoscale patterns in an ultra-fast and highly reproducible manner. Although sphere-to-plate geometry was used in this experiment, other shaped confinements (e.g. pyramid-on-flat) should also be applicable, yielding rich nanoscale structures.

Acknowledgments

This work was supported by the National Key Basic Research Program of China (Grant No. 2011CB933503), Basic Research Program of Jiangsu Province (Natural Science Foundation) (Grant Nos BK2011036, BK2009013) and China–US International Science and Technology Cooperation Program (Grant No. 2009DFA31990).

References

[1] Sargent E H 2012 *Nature Photon.* **6** 133
[2] Fuechsle M, Miwa J A, Mahapatra S, Ryu H, Lee S, Warschkow O, Hollenberg L C L, Klimeck G and Simmons M Y 2012 *Nature Nanotechnol.* **7** 242
[3] Alivisatos P 2004 *Nature Biotechnol.* **22** 47
[4] Biswas A, Bayer I S, Biris A S, Wang T, Dervishi E and Faupel F 2012 *Adv. Colloid Interface Sci.* **170** 2
[5] Rabani E, Reichman D R, Geissler P L and Brus L E 2003 *Nature* **426** 271
[6] Velev O D and Gupta S 2009 *Adv. Mater.* **21** 1897
[7] Zhang J, Li Y, Zhang X and Yang B 2010 *Adv. Mater.* **22** 4249
[8] Liao W-S, Chen X, Chen J and Cremer P S 2007 *Nano Lett.* **7** 2452
[9] Love J C, Estroff L A, Kriebel J K, Nuzzo R G and Whitesides G M 2005 *Chem. Rev.* **105** 1103
[10] Huang J, Fan R, Connor S and Yang P 2007 *Angew. Chem. Int. Edn* **46** 2414
[11] Hong S W, Byun M and Lin Z 2009 *Angew. Chem. Int. Edn* **48** 512
[12] Hong S W, Wang J and Lin Z 2009 *Angew. Chem.* **121** 8506
[13] Hong S W, Xu J, Xia J, Lin Z, Qiu F and Yang Y 2005 *Chem. Mater.* **17** 6223
[14] Kim M H, Im S H and Park O O 2005 *Adv. Funct. Mater.* **15** 1329
[15] Lin Z and Granick S 2005 *J. Am. Chem. Soc.* **127** 2816
[16] Xu J, Xia J, Hong S W, Lin Z, Qiu F and Yang Y 2006 *Phys. Rev. Lett.* **96** 066104
[17] Xu J, Xia J and Lin Z 2007 *Angew. Chem.* **119** 1892
[18] Diao J J, Hutchison J B, Luo G and Reeves M E 2005 *J. Chem. Phys.* **122** 184710
[19] Murisic N and Kondic L 2011 *J. Fluid Mech.* **679** 219
[20] Baghbanzadeh M, Carbone L, Cozzoli P D and Kappe C O 2011 *Angew. Chem. Int. Edn* **50** 11312
[21] Hu X, Yu J C, Gong J, Li Q and Li G 2007 *Adv. Mater.* **19** 2324
[22] Wang H, Zhang J-R and Zhu J-J 2001 *J. Cryst. Growth* **233** 829
[23] Druzhinina T, Weltjens W, Hoeppener S and Schubert U S 2009 *Adv. Funct. Mater.* **19** 1287
[24] Kim S-H, Lee S Y, Yi G-R, Pine D J and Yang S-M 2006 *J. Am. Chem. Soc.* **128** 10897
[25] Pozar D M, Targonski S D and Syrigos H D 1997 *IEEE Trans. Antennas Prop.* **45** 287
[26] Olgun U U 2009 *ACS Appl. Mater. Interfaces* **2** 28
[27] Park S-J, Taton T A and Mirkin C A 2002 *Science* **295** 1503
[28] Shanahan M E R 1995 *Langmuir* **11** 1041
[29] Lin Z 2010 *J. Polym. Sci.* B **48** 2552
[30] Myunghwan B, Jun W and Zhiqun L 2009 *J. Phys.: Condens. Matter* **21** 264014
[31] Deegan R D 2000 *Phys. Rev.* E **61** 475
[32] Sultan E, Boudaoud A and Amar M B 2005 *J. Fluid Mech.* **543** 183
[33] Maheshwari S, Zhang L, Zhu Y and Chang H-C 2008 *Phys. Rev. Lett.* **100** 044503
[34] Perelaer J, de Gans B J and Schubert U S 2006 *Adv. Mater.* **18** 2101
[35] Kakefuda Y, Narita K, Komeda T, Yoshimoto S and Hasegawa S 2008 *Appl. Phys. Lett.* **93** 163103